Knowledge-Based Systems xxx (xxxx) xxx–xxx

Contents lists available at ScienceDirect

Knowledge-Based Systems

journal homepage: www.elsevier.com/locate/knosys

Multistep-ahead forecasting of chlorophyll *a* using a wavelet nonlinear autoregressive network

Du Zhenhong[a,b,*], Qin Mengjiao[a,b], Zhang Feng[a,b], Liu Renyi[a,b]

[a] School of Earth Sciences, Zhejiang University, Hangzhou 310027, China
[b] Zhejiang Provincial Key Laboratory of Geographic Information Science, Hangzhou 310028, China

ARTICLE INFO

Keywords:
Multistep-ahead forecasting
WNARNet
Wavelet transform
NAR
Chlorophyll *a* forecasting

ABSTRACT

Multistep-ahead forecasting is essential to many practical problems, such as the early warning of disasters. However, existing studies mainly focus on current-time or one-step-ahead prediction since forecasting multiple steps continuously presents difficulties, such as accumulated errors and long-term time series modeling. In this paper, an effective multistep-ahead forecasting model wavelet nonlinear autoregressive network (WNARNet), which integrates the wavelet transform and a nonlinear autoregressive neural network (NAR), is proposed for the forecast of chlorophyll *a* concentration. The wavelet transform decreases the accumulative errors by dividing complicated time series into simpler ones. Simultaneously, the NAR maintains the dependencies between the time series. The buoy monitoring data of the Wenzhou coastal area obtained in 2014-2015 is used to verify the feasibility and effectiveness of WNARNet. The model performs well in predicting the dynamics of chlorophyll *a* and it is able to predict different horizons flexibly and accurately without training new models. Furthermore, experimental results demonstrate that WNARNet significantly outperforms other benchmark methods of multistep-ahead forecasting. When forecasting 20 steps ahead, the r of WNARNet is 0.08 higher and the RMSE is 0.04 lower than the values of the benchmark models. Therefore, the newly proposed approach represents a promising and effective method for the future prediction of chlorophyll *a*.

1. Introduction

Harmful algal blooms (HABs), which arise from a variety of environmental problems, including eutrophication [1], climate change [3] and water pollution [4], have become one of the most serious costal disasters, posing threats to the ecosystem and human health. We are at a crossroads with regard to controlling HABs and must aggressively address this problem before it becomes more severe [2]. Chlorophyll *a* (*Chl a*) concentration is usually used to indicate the algal bloom intensity (e.g., [5,6]). Therefore, this paper focuses on the time series forecasting of *Chl a*, which is of great significance in the control and prediction of HABs.

The *Chl a* concentration is closely related to the intensity of algal blooms. When HABs occur, the *Chl a* concentration increases sharply and has many mutations, making it challenging to forecast *Chl a*. Existing studies are mainly devoted to forecasting *Chl a* few steps ahead or to fitting the current *Chl a* data to other environmental factors. For example, autoregressive integrated moving average (ARIMA) was used to predict *Chl a* one step ahead [5]; a wavelet neural network (WNN) was proposed to forecast *Chl a* series three steps ahead [6]; and a wavelet-based fuzzy model forecasted *Chl a* based on water quality and hydrological variables [7]. To help in the early warning of HABs, it is urgent to design a new model to accurately forecast *Chl a* multiple steps ahead.

Multistep-ahead forecasting refers to the continuous prediction of multiple future steps ahead. In this paper, the number of consecutive predicted steps is termed the forecasting horizon. Compared with one-step-ahead forecasting, multistep-ahead forecasting is more useful but also challenging because it has to address various additional complications, such as accumulation of errors, model complexity, and increased uncertainty [8,9]. Currently, there are three major strategies for addressing the multistep-ahead forecasting problem: the recursive strategy, the direct strategy and the joint strategy [10].

The recursive strategy is based on one-step-ahead forecasts. The *h*th step ahead is forecasted using previously forecasted values as inputs. ARIMA [5] models and seasonal autoregressive integrated moving average (SARIMA) models [11] are commonly used traditional methods. However, they are flawed in forecasting nonlinear and nonstationary series. With the development of artificial intelligence, machine learning has become the mainstream approach to compensate for

* Corresponding author at: Zhejiang Provincial Key Laboratory of Geographic Information Science, Xixi Campus Zhejiang University, Hangzhou 310007, China.
E-mail addresses: duzhenhong@zju.edu.cn (Z. Du), qinmengjiao@zju.edu.cn (M. Qin), zfcarnation@zju.edu.cn (F. Zhang), liurenyi@zju.edu.cn (R. Liu).

https://doi.org/10.1016/j.knosys.2018.06.015
Received 2 November 2017; Received in revised form 25 June 2018; Accepted 28 June 2018

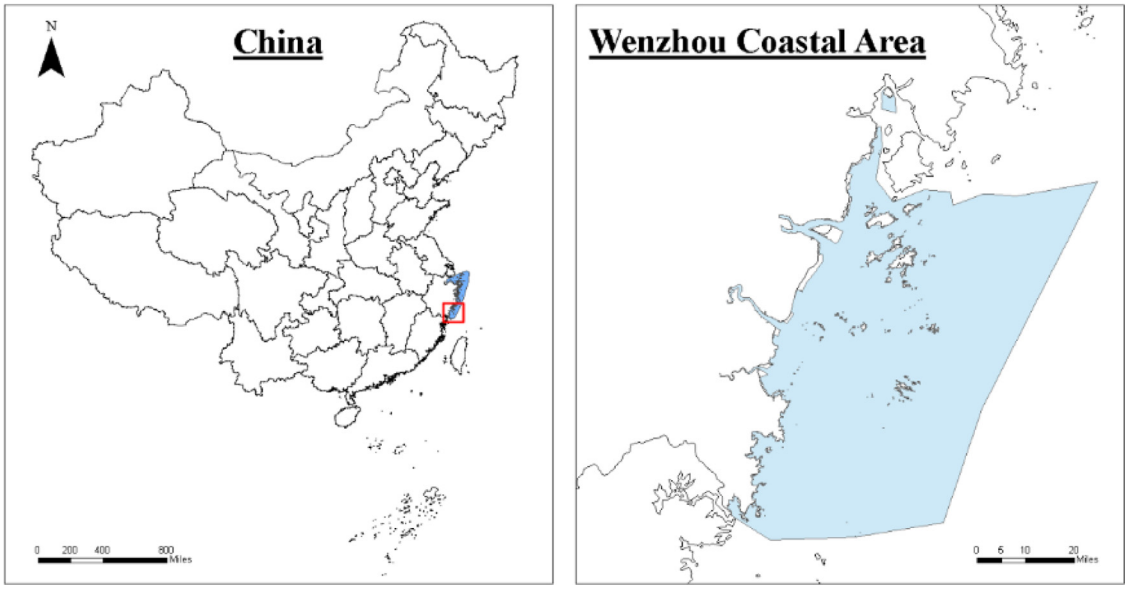

Fig. 1. Study area map. Wenzhou coastal area, Zhejiang Province, China.

the lack of traditional methods and has achieved great success. For example, a nonlinear recurrent neural network (NRNN) was proposed for multistep forecasting of wave power [12]; a WNARX model was developed for real-time flood forecasting [13]; and NAR was applied to forecasting small-scale solar radiation [14]. Nevertheless, the recursive strategy methods suffer from accumulated errors. Hence, with the increase in the forecasting horizon, the prediction accuracy further declines.

For the direct strategy, different forecasting models are trained to directly forecast each *h*th step ahead. Artificial neural network (ANN)-based models are the most popular direct strategy methods and have been used in various fields, such as financial prediction [15], algal bloom forecasting [6], wind speed forecasting [16] and oil production prediction [17]. In addition, fuzzy inference systems, such as the TS-fuzzy model [18], adaptive network-based fuzzy inference system (ANFIS) [19,20], extreme learning machine (ELM) [21,22], support vector machine (SVM) [23], fuzzy cognitive map (FCM) [24], deep belief network (DBN) [25] and hidden Markov model [26], are popular direct strategy methods.

However, when the forecasting horizon is large, e.g., 20, these methods need to train 20 different models to forecast each step separately. The correlations between the forecasted values are lost, and the cost of model training is high. Thus, most of the direct strategy approaches are intended to forecast one step or a few steps ahead rather than long-term predictions.

In the joint strategy, a multi-output model is designed to forecast the whole horizon in one shot. Commonly used approaches include multi-output NNs [27], multi-output SVRs [28,29], and the multi-output stochastic frontier approach [30]. Since the output dimension is fixed, the joint strategy methods have to train new models once the forecasting horizon is changed. Furthermore, when the forecasting horizon becomes larger, the accuracy of the model will greatly decline. As a result, the models with high output dimensions are hard to train.

Overall, the three strategies all have some challenges that need to be addressed. To accurately predict the *Chl a* time series, an efficient recursive-joint strategy approach, WNARNet, is proposed in this paper. The wavelet transform and a nonlinear autoregressive neural network (NAR) are integrated in the new model. First, one-level wavelet transform is used to divide the original series into two frequencies. The *Chl a* series is nonlinear and nonstationary due to the mutations and irregular increases during the HABs. Wavelet transform can help decompose the complex series into simpler ones and alleviate the difficulty of model fitting. Then, a two-pathway NAR is applied to forecast the decomposed series derived from the wavelet transform. The NAR, as a type of recurrent dynamic network, is powerful for modeling and forecasting nonlinear time series through past values, and no auxiliary data are needed. Moreover, the NAR can forecast different horizons flexibly without training new models. Finally, the forecasted values obtained from the two-pathway NAR are aggregated to reconstruct the final forecasting series through inverse wavelet transform. The contributions of this paper are as follows:

(1) An efficient multistep-ahead forecasting model WNARNet, which combines the wavelet transform and NAR, is proposed in this paper, and it is shown that the model can flexibly forecast different horizons without training new models from scratch.
(2) WNARNet is able to forecast two values in one shot with the two-pathway NARs, resulting in a significant reduction in the cumulative error.
(3) Wavelet transform is employed to divide a complicated time series problem into simpler ones, which alleviates the difficulty of model fitting and improves model performance.

The remainder of this paper is organized as follows: Section 2 introduces the materials and methods used in this work for the multistep-ahead forecasting of *Chl a*, and a background of the discrete wavelet transform and NAR methods is reviewed. In Section 3, we present the multistep-ahead forecasting results of the proposed method and compare the results with those obtained by other state-of-the-art approaches, including ANN, ARIMA, NAR and WNN. In Section 4, the utility and the characteristics of the proposed model are discussed. The last section is devoted to summarizing this work.

2. Materials and methods

2.1. Study area and data collection

Our experiment is based on a real dataset of the Wenzhou coastal area (27°03′–28°21′N, 120°25′–121°50′E), Zhejiang Province, China, as shown in Fig. 1. Due to the mariculture and water pollution, the nutrient concentration in the water has increased, which favors the reproduction of harmful algae. The Wenzhou coastal area is sensitive to HABs and has suffered from HABs since the 1990s [31]. Simultaneously, *Chl a* increases irregularly and undergoes many mutations

during the occurrences of HABs. Therefore, the Wenzhou coastal area was chosen for our case study to evaluate the effectiveness and practicability of the proposed approach.

A real-time online monitoring system with an on-site buoy and an onshore data center was constructed in the Wenzhou coastal area in 2013. The buoy continuously monitors water quality, meteorological conditions and nutritional conditions using different sensors. Since the buoy began its operation, it has detected many HAB events. The monitoring parameters include *Chl a* concentration, temperature, dissolved oxygen, salinity, and others. Monitoring data from the buoy are transferred back to the data center every 30–60 min. *Chl a* concentration is quantified at 0.2–0.5 m below the water surface with a resolution of 0.01 μg L^{-1}. The hourly values of *Chl a* concentration from 1 Jan. 2014 to 30 Dec. 2015 are analyzed in this study, and the data interval is 1–2 hours. All the data are provided by Public Science and Technology Research Funds' Projects (PSTRFP) and are in the form of spreadsheets.

2.2. Wavelet nonlinear autoregression network

2.2.1. Discrete wavelet transform

Wavelet analysis is a tool for the representation, decomposition and reconstruction of signals [16]. This algorithm was first proposed by Mallat [32] and has been used in various fields, such as signal analysis [33], image processing [34], remote sensing data decomposition [35], and medical imaging and diagnosis [36]. The discrete wavelet transform, as a kind of wavelet analysis algorithm, is able to transform the signals into time-frequency domains and decompose the signals to one approximation set and several detailed sets. The original time series is written as $S = [s(0),...,s(N-1)]$ with $k = 0, 1, ...,N-1$ and $N = 2^J$. The discrete wavelet transform can be written as Eqs. (1) & (2):

$$W_\varphi(j_0, n) = \frac{1}{\sqrt{N}} \sum_k s(k)\varphi_{j_0,n}(k) \tag{1}$$

$$W_\psi(j, n) = \frac{1}{\sqrt{N}} \sum_k s(k)\psi_{j,n}(k) \tag{2}$$

where $j_0 = 0, j = 0, 1, ...,J-1$ and $n = 0, 1, ...,2^j - 1$. The elements ψ and φ are the wavelet function and the scaling function, respectively. The reconstruction of the original series is written as Eq. (3):

$$s(k) = \frac{1}{\sqrt{N}} \sum_n W_\varphi(j_0, n)\varphi_{j_0,n}(k) + \sum_{j=j_0}^{\infty} \sum_n W_\psi(j, n)\psi_{j,n}(k) \tag{3}$$

For a precise forecast of *Chl a* concentrations, the original *Chl a* series is processed using the discrete wavelet transform. Several wavelet families can be used, e.g., Daubechies (dbN), Coiflets (coifN) and Symlets (symN). In this work, db1 is chosen to decompose the original series into one approximation set (A) and one detail set (D). Fig. 2 shows the original series and the two series obtained from the discrete wavelet transform.

2.2.2. Nonlinear autoregression neural network

Nonlinear autoregression networks (NARs) have been widely used in time series forecasting, such as solar radiation forecasting [14,37], prediction of building's energy consumption [38], short-term load forecasting [39] and wave power prediction [12]. NAR is a recurrent dynamic network based on a linear autoregressive model with feedback connections, including an input layer, an output layer and several hidden layers. As shown in Eq. (4), the past values of the time series are used as the input to predict the future values:

$$y'_t = f(y_{t-1} + y_{t-2}+...+y_{t-d}) \tag{4}$$

Here, f is a nonlinear function, and d is the time delay parameter, meaning that the future values depend only on the previous d values ($y_{t-1}, y_{t-2}, ...,y_{t-d}$). Fig. 3 provides a specific description of the structure and forecasting process of NAR.

In this study, a two-pathway NAR must be trained for the approximation (A) and detail (D) sets, respectively. A and D are transformed from the original *Chl a* time series using the discrete wavelet transform. Back-propagation through time with a stochastic gradient descent is used to train the model.

2.2.3. Multistep-ahead forecasting model WNARNet

An efficient multistep-ahead forecasting method is proposed in this study by combining the wavelet transform and nonlinear autoregressive networks. The so-called wavelet nonlinear autoregressive network (WNARNet) can be outlined in the following steps:

Step 1: decomposition of the original time series into low frequency (approximation set) and high frequency (detail set) using the one-level discrete wavelet transform;
Step 2: construction of two-pathway NAR for the two decomposed series;
Step 3: multistep-ahead forecasting of each decomposed series with the two-pathway NAR;
Step 4: the individual output series from the two-pathway NAR are recomposed to form the predicted series (Fig. 4) through inverse wavelet transform.

In this study, the parameters of WNARNet for multistep-ahead forecasting of *Chl a* are designed as follows.

First, the original *Chl a* time series is decomposed into two series using the db1 wavelet. The first series is the approximation set (A), and the second series is the detail set (D). Then, two NARs need to be trained to model and forecast A & D. Since the length of the decomposed series (A/D) is half of the original series, the time delay (d) and the forecasting horizon (H) for each series is halved as well (Fig. 2). Finally, the outputs of the two-pathway NARs are aggregated to reconstruct the simulations of the original series.

To obtain the best NARs, the number of hidden layers (n) is designated as 1 or 2. This is because if n is large, NAR is more likely to overfit, resulting in inaccurate prediction with large bias. Each hidden layer has multiple neurons to learn the features of data. Experimental data from 2014 are used to train the model, and data from 2015 are used for testing. The structure with the smallest testing error is taken to be the best structure of NAR for *Chl a* time series forecasting.

2.3. Model evaluation

2.3.1. Evaluation criteria

The correlation coefficient (r), root mean squared error (*RMSE*) and mean absolute error (*MAE*) are used to evaluate the predictive ability of the predictive model.

$$\begin{cases} r = \dfrac{\sum_{t=1}^{N}(y_t-\bar{y})(y'_t-\overline{y'})}{\sqrt{\sum_{t=1}^{N}(y_t-\bar{y})^2}\sqrt{\sum_{t=1}^{N}(y'_t-\overline{y'})^2}} \\ RMSE = \sqrt{\dfrac{\sum_{t=1}^{N}(y_t-y'_t)^2}{N}} \\ MAPE = \frac{1}{N}\sum_{t=1}^{N}\left|\dfrac{y_t-y'_t}{y_t}\right| \times 100\% \end{cases} \tag{5}$$

Here, t is the time, y_i is the actual value, y'_i is the predicted value, and $\bar{y}$ and $\overline{y'}$ are the means of y_t and y'_t ($t = 1, 2, ...,N$), respectively.

The important properties of the above three evaluation criteria are as follows:

r quantifies the strength of the correlation between the actual series and the prediction series. The range of r is [0, 1], and values closer to 1 correspond to better correlation of the forecasting model.

RMSE is the square root of the calculated mean squared error (*MSE*), which measures the average squared deviation of forecasted values and provides an overall measure of the error in the forecasting. RMSE is also sensitive to the changes in scale and data transformations.

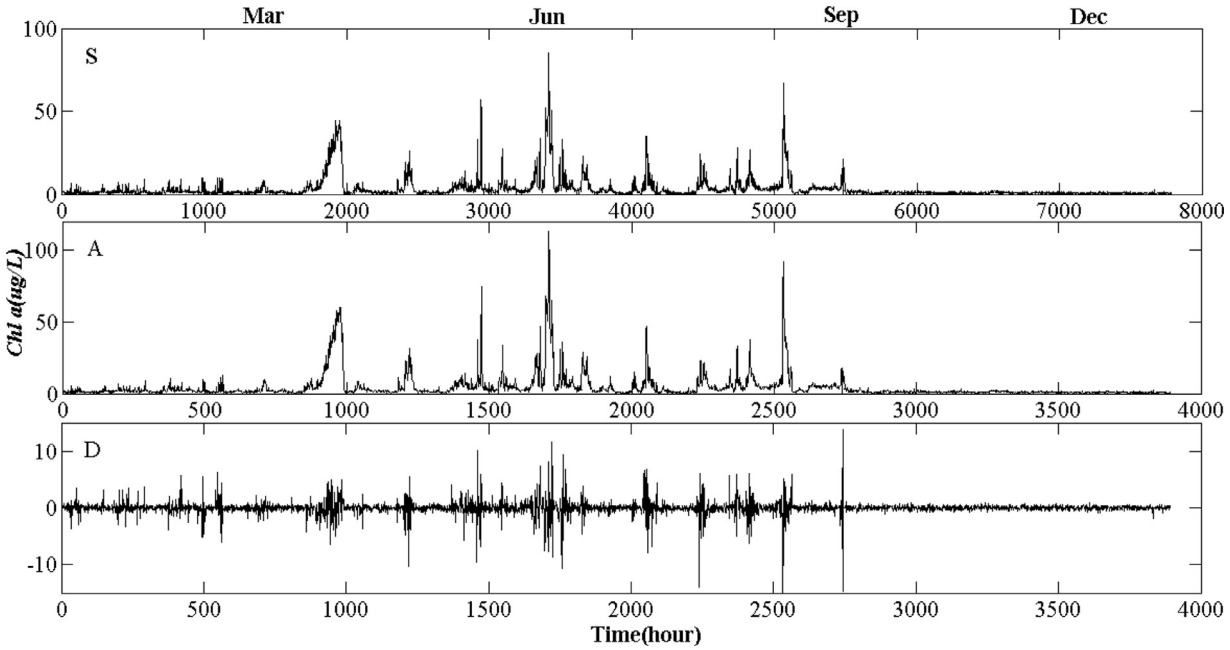

Fig. 2. Wavelet decomposition of the hourly *Chl a* time series in the Wenzhou coastal area. S is the original signal in 2015, and the approximation series plot (A) and the detailed series plot (D) are obtained using the db1 wavelet.

MAPE measures the percentage of average absolute error relative to the real value. It is independent of the scale of measurement but is affected by data transformation. The obtained MAPE should be as small as possible for a good forecast.

RMSE and *MAPE* are commonly used to measure the performance of the model. In this work, they are used to evaluate the forecasting accuracy of WNARNet. RMSE and MAPE values closer to 0 imply higher accuracy of the model. Additionally, these three criteria can be applied to compare different models.

2.3.2. Comparison approaches

The approaches employed for algorithm comparison can be roughly divided into two categories. The first category is to compare the influences of different parts of the proposed approach and to illustrate the motivation of combining the wavelet transform and nonlinear autoregressive network. The methods used for the comparison include NAR [12] and the wavelet neural network (WNN) [6]. The second category is to compare the proposed model with the state-of-the-art approaches, such as ARIMA [5], ANN [40], WNN and ANFIS models [20]. The principles and structure of NAR are the same as those described in Section 2.2.2. The general description of the ARIMA(p,d,q) model is shown in Eq. (6):

$$y_t = a_t + \varphi_1 y_{t-1} + \varphi_2 y_{t-2} + \ldots + \varphi_p y_{t-p} - \varepsilon_t - \theta_1 \varepsilon_{t-1} - \theta_2 \varepsilon_{t-2} - \ldots - \theta_q \varepsilon_{t-q} \tag{6}$$

where y is the original series obtained by taking the difference d times; φ_1, φ_2, $\ldots\varphi_p$ and $\theta_1, \theta_2, \ldots\theta_q$ are the calculated autoregressive and moving-average coefficients, respectively; and ε_t, ε_{t-1}, $\ldots\varepsilon_{t-q}$ are assumed to be independently and identically distributed with the mean of zero and a constant variance.

For ANN and ANFIS, the direct strategy is used for multistep-ahead forecasting. Hence, different models are trained for each step of forecasting. If the horizon is H, then H different models are needed. Furthermore, the back-propagation algorithm is used when training the models. ANFIS is based on artificial neural networks and the Takagi–Sugeno fuzzy inference system. It can automatically generate a set of If-Then rules that have the capability to approximate nonlinear functions.

WNN combines wavelet analysis and the artificial neural network. The original series is first decomposed by the discrete wavelet transform, and each decomposed series is used as input to an individual ANN for forecasting. Then, the individual output series from these networks are recomposed to form the forecasted series. There is a great difference between our model (WNARNet) and WNN, especially for multistep-ahead forecasting. WNN is a direct strategy like the ANN model, and WNARNet is based on the recursive-joint strategy. Therefore, when the forecasting horizon is H, WNN needs to train H/2 networks for each

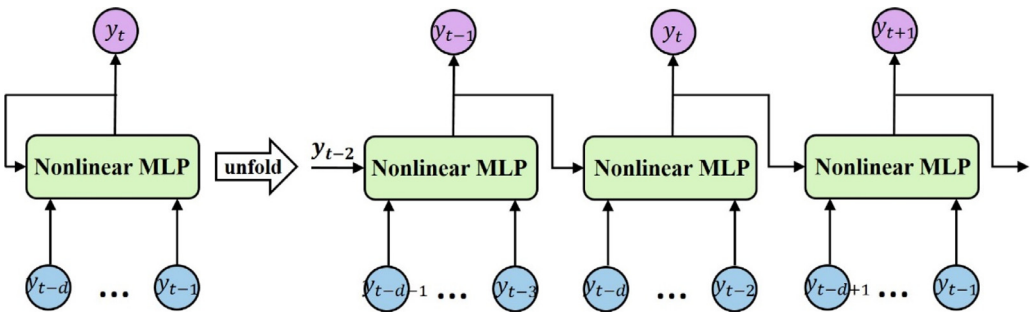

Fig. 3. Architecture of a nonlinear autoregressive neural network (NAR). MLP means multi-layer perceptron. NARs consist of an input layer, several hidden layers (nonlinear multi-layer perceptron) and an output layer. The previous output values are taken as the input of next step in the model to forecast the new values.

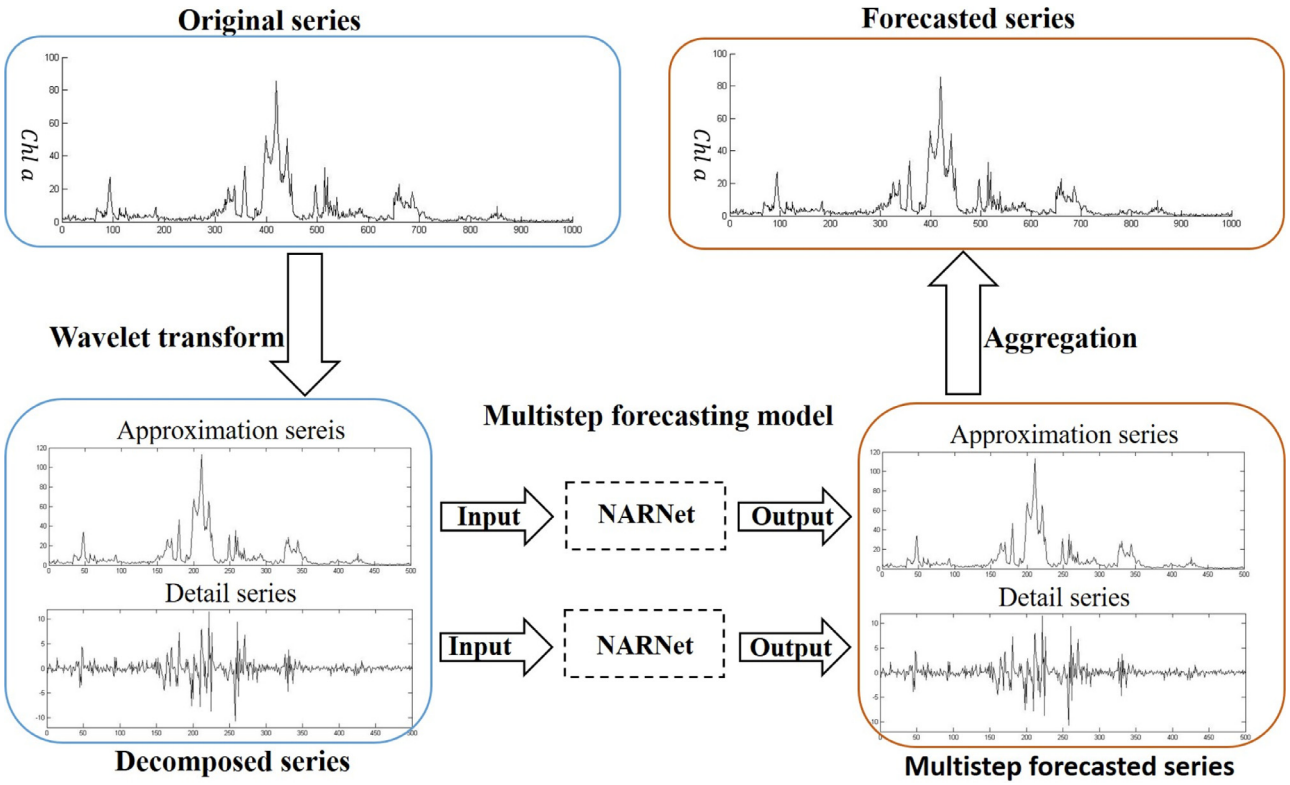

Fig. 4. Diagrammatical representation of the hybrid process of wavelet transform and NAR. The specific procedure of WNARNet is 1) the original series is transformed into an approximation series (A) and a detail series (D) by wavelet transform (*Step 1*); 2) a two-pathway NARs is constructed for multistep forecasting of the A and D separately (*Step 2* & *Step 3*); and 3) the forecasted series of A and D are summed to reconstruct the final forecasting series (*Step 4*).

decomposed series, while WNARNet only needs to train one model.

Since the strategies are not the same, we compare not only the forecasting performance of the whole horizon but also the r and errors of each hth step (h = 1,…,H). The input and output of all the models are consistent with WNARNet.

The specific differences between the models in multistep-ahead forecasting are shown in Table 1.

3. Results

3.1. Multistep-ahead forecasting results with WNARNet

The original time series (S) of hourly *Chl a* concentration in the Wenzhou coastal area in 2015 (Fig. 2) shows strong mutations and non-stationarity. The discrete wavelet transform based on the db1 wavelet was used to decompose the series (S) into an approximation series (A) and a detail series (D). The approximation series A focuses on describing the global information. As shown in Fig. 2, A indicates that the *Chl a* series has obvious seasonal characteristics, i.e., the *Chl a* concentration is low during the winter (October-December). In March, small peaks appear, showing that the algal population is recovering. There are many peaks and mutations from May to September, demonstrating that bloom events occur in the summer and autumn. Meanwhile, D is the detailed information of high frequency, and larger variability is observed in D than in A or S.

Table 1
Specific differences between the models.

Algorithm	Number of networks for horizon = H	Strategy
ARIMA	–	Recursive
ANN	H	Direct
NAR	1	Recursive
WNN	H	Direct
WNARNet	2	Recursive-joint
ANFIS	H	Direct

The multistep-ahead forecasting with WNARNet contains two components: the training component and the prediction component. The series in 2014 is applied to the training of the model, and the series in 2015 serves to verify the forecasting performance of the optimal model.

During the training process, each 22 continuous frames of data make up a training sample, in which the first 20 frames are used as the input to WNARNet and the last two frames are the ground truth (target values). Specifically, the input series is first decomposed into A and D by the wavelet transform, and then A and D are fed into a two-pathway NAR to obtain predicted values. Next, the forecasted values of the two-pathway NARs are aggregated to reconstruct the final forecasting values. Finally, WNARNet can be trained recursively through minimizing the error between the predicted value and ground truth. The grid search method is used as the tuning method to obtain the best parameters. As shown in Supplementary Table A1 through Table A4, the best structures for A and D are (3, 6) and (7, 7), respectively (the first coordinate is the number of units of the first hidden layer, and the second coordinate is the number of units of the second hidden layer). For the prediction process, the forecasting horizon can be set as any positive value since the predicted value of the previous step serves as the input of the model in the next step. In this paper, the optimal WNARNet is used to forecast *Chl a* series with the forecasting horizon of 20 used as an example.

The results of WNARNet suggest that the simulations are highly accurate, as shown by the calculated R, RMSE and MAPE values (Table 2). The R value is higher than 0.952, and the errors are very small (RMSE = 2.010 μg L^{-1} and MAPE = 0.375) when forecasting one step ahead. Table 2 shows the results of each step when the horizon is 20. It is apparent that as the prediction step increases, the accuracy is gradually reduced because the predicted values at the previous step are

Table 2
Multistep-ahead forecasting performance of WNARNet.

	*h*th step (horizon = 20)[a]			Horizon[b]		
	r	RMSE (μg L^{-1})	MAPE	r	RMSE (μg L^{-1})	MAPE
1	0.952	2.010	0.375	0.952	2.010	0.375
2	0.923	2.417	0.372	0.938	2.213	0.374
3	0.922	2.615	0.494	0.932	2.347	0.414
4	0.885	2.935	0.528	0.920	2.494	0.442
5	0.880	3.199	0.650	0.912	2.635	0.484
6	0.856	3.328	0.670	0.903	2.751	0.515
7	0.851	3.593	0.762	0.896	2.871	0.550
8	0.824	3.653	0.818	0.887	2.969	0.584
9	0.818	3.945	0.904	0.879	3.077	0.619
10	0.795	3.975	0.920	0.871	3.167	0.649
11	0.795	4.190	1.026	0.864	3.260	0.684
12	0.777	4.145	0.975	0.857	3.334	0.708
13	0.777	4.366	1.073	0.850	3.413	0.736
14	0.759	4.341	1.086	0.844	3.479	0.761
15	0.758	4.562	1.185	0.838	3.552	0.789
16	0.745	4.463	1.131	0.832	3.609	0.811
17	0.745	4.677	1.220	0.827	3.671	0.835
18	0.731	4.624	1.229	0.822	3.724	0.857
19	0.731	4.848	1.325	0.817	3.783	0.881
20	0.722	4.696	1.266	0.812	3.829	0.901

[a] Each step of forecasting performance of WNARNet when the horizon is 20.
[b] Multistep-ahead forecasting performance of the WNARNet with horizons from 1 to 20.

taken as the input of the next step in the model to forecast the latter steps, which results in error accumulation. Although the forecasting accuracy decreases with increasing step number, the accuracy of WNARNet is much higher than that of the other approaches. For instance, when predicting the 10th step, the r of WNARNet is 0.795, while those for the other algorithms are all lower than 0.75. The advantages of WNARNet are maintained quite well as the steps increase. Even for the 20th step, the r is higher than 0.70.

The one-step-ahead predicted values and the actual values are shown in Fig. 5(a). Furthermore, to evaluate the performance of the proposed model for peak prediction, we zoom to June, as shown in Fig. 5(b). In June 2015, the *Chl a* concentration reaches the highest value (85.40 μg L^{-1}), and there are obvious mutations during this month. The visual comparison of the actual and predicted values confirms the validity of WNARNet in the forecasting of algal dynamics. Fig. 5 shows that the proposed model can successfully predict the hidden pattern of the original observed data, and almost all the peak values can be precisely forecasted, which is of great significance for providing early warning of HABs.

3.2. Different horizons

To assess the effectiveness and practicality of the developed WNARNet for different horizon predictions, the forecast is applied to the horizons varying from 1 to 20. Due to the advantages and characteristics of the recursive strategy, it is not necessary to train new models to perform the entire forecasting; rather, the optimal model obtained from Section 3.1 is sufficient.

The results shown in Table 2 reveal that WNARNet is able to forecast different horizons flexibly and accurately. Even for the prediction of 20 consecutive steps ahead, the average r (0.812) of the whole horizon is higher than 0.8. Specifically, with the increase in the horizon, the r of the whole horizon decreases, while the MAPE and RMSE rise. This is due to the additive or accumulative effect of forecast error in the absence of a corrective mechanism [10].

3.3. Comparison of WNARNet with state-of-the-art approaches

In this part, WNARNet is compared with five state-of-the-art forecasting approaches: the ARIMA, NAR, ANN, WNN and ANFIS models. All of the approaches are constructed on the hourly dataset of *Chl a* in the Wenzhou coastal area, as used in Section 3.1. The input dimension of these models is 20, corresponding to the past 20 values. The parameters and architectures of all approaches are listed in Table 3. For the neural networks (i.e., NAR, ANN, WNN and WNARNet), the numbers of inputs, outputs and hidden nodes are presented. In terms of ANFIS and ARIMA, the important parameters are shown in the table.

Figs. 6 and 7 present the comparison results of multistep-ahead forecasting. An in-depth analysis of the performance of multistep-ahead forecasting approaches can be accomplished by experimenting with different horizons. Hence, all models are used for forecasting with the horizon varying from 1 to 20. Furthermore, we reveal the difference between the recursive and direct strategies by analyzing the accuracy of each *h*th step predicted values when the horizon is 20.

The results of the multistep-ahead forecasting performance of the models for different horizons are shown in Table 4 and Fig. 6. Due to space limitations, Table 4 only lists the details of the comparison results for the horizons of 1, 10 and 20. As revealed in the table, WNARNet shows the best performance in multistep-ahead forecasting of a *Chl a* time series. On the one hand, the results of NAR and ANN are slightly better than those of WNARNet for the horizon of 1 (r(NAR) = 0.954, r(ANN) = 0.956, r(WNARNet) = 0.952). On the other hand, WNARNet achieves the largest r and the smallest RMSE and MAPE when the horizon increases. In addition, Fig. 6 shows that with the increase in the horizon, the r of the proposed model is better than that for the other models, illustrating that the proposed method not only correctly predicts short-term values but also works well in long-term prediction.

Furthermore, WNARNet is very flexible and easy to extend to different horizons without training the new model from scratch. As shown in Table 1, WNN, ANN and ANFIS need to train 20 different networks when the horizon is 20, while WNARNet only needs to train two networks. Although NAR needs only one network, and three parameters are needed for the ARIMA model, they show much worse results than our proposed model. Overall, WNARNet is a more powerful and more flexible method than the other methods in terms of multistep-ahead forecasting.

For the horizon of 20, a visual comparison of the forecasting performance of all algorithms at each step is presented in Fig. 7. By analyzing the characteristics of the curves in the figure, it is easy to understand the differences in the different multistep-ahead forecasting strategies and see the origin of the advantages exhibited by WNARNet.

First, compare the differences between recursive strategy approaches and direct strategy approaches. For recursive strategy-based methods, such as ARIMA, NAR and WNARNet, the values obtained later are worse than the previous forecasted values because of the accumulated error (Fig. 7). Among the three models, the results of ARIMA are the worst, showing the smallest r and the largest RMSE. This is because ARIMA is a linear model that is not able to address the nonlinear and nonstationary series.

Unlike the recursive strategy methods, there is no correlation between the steps of the WNN, ANN and ANFIS methods because they separately forecast each step ahead. For the direct strategy methods, it is possible that the latter forecasted values are more accurate than the previous forecasted values. As Fig 7 shows, the MAPE curves of these three approaches are not as smooth and stable as the others. The MAPE of the 15th step (4.367) of ANN is the highest, and the MAPE results of ANFIS after the 17th step are smaller than those from the 4th-16th steps. Moreover, the r of the 7th step (0.787) of the WNN model is larger than that of the 6th step (0.780). Since different models are trained for different step forecasts, the direct strategy successfully avoids the risk of generating cumulative errors. Hence, the forecasting performances of WNN and ANN are better than those of NAR and ARIMA, especially in terms of the RMSE. However, since each *h*th step is forecasted in isolation from the other steps, the strategy could produce completely unrelated forecasts over the whole horizon, possibly

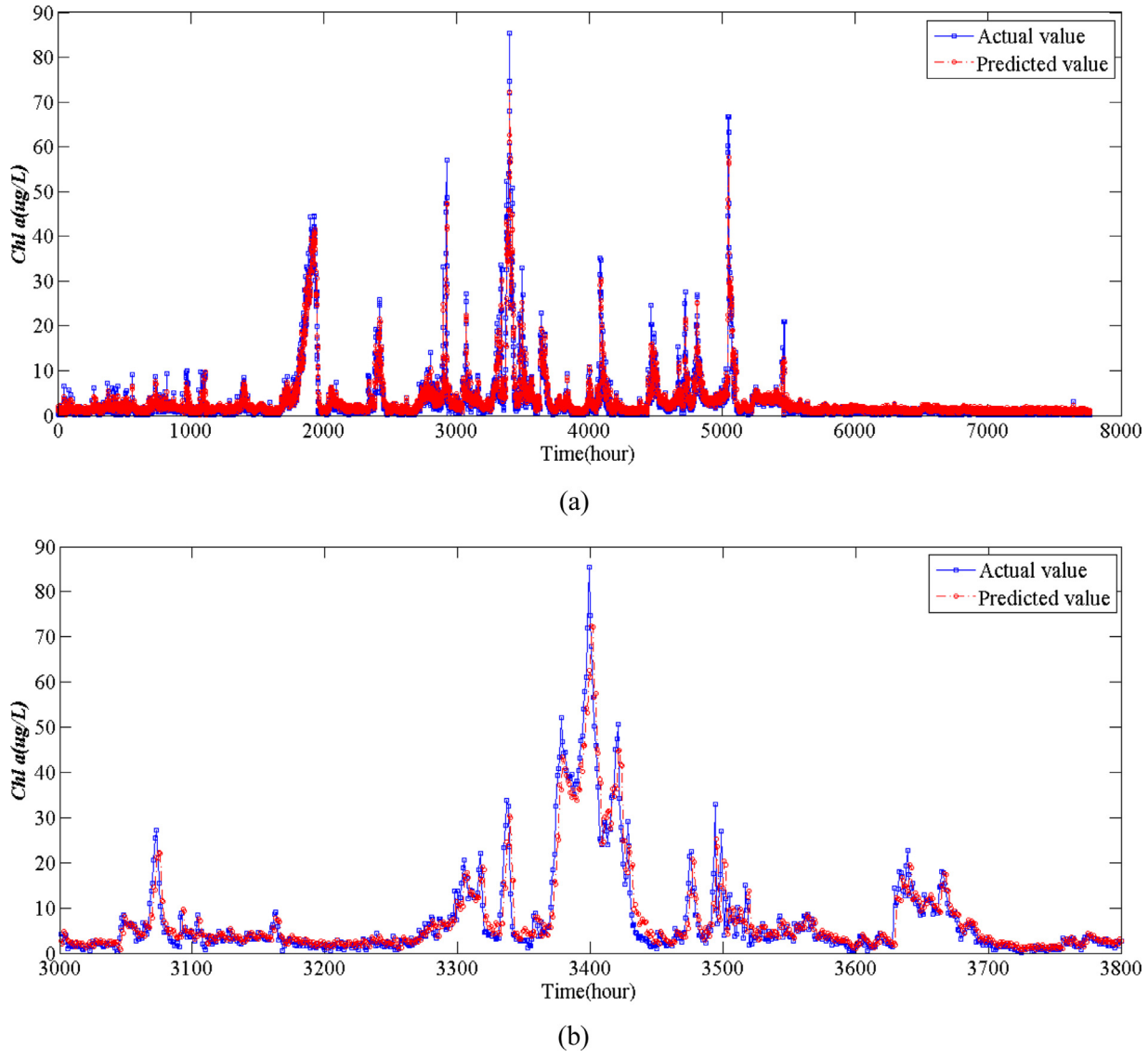

Fig. 5. One-step-ahead forecasting results of *Chl a* with WNARNet. (a) Shows results for the whole year of 2015, and (b) zooms to June 2015 to focus on the performance for peak prediction.

Table 3
The parameters and architectures of algorithms.

Algorithm	Structure of models[a]		
	Input layer	Hidden layers	Output layer
NAR	20	(6,6)	20
ANN	20	(10,6)	1
WNN	$(10)_A$ $(10)_D$	$(10,4)_A$ $(8,3)_D$	$(1)_A$ $(1)_D$
WNARNet	$(10)_A$ $(10)_D$	$(3,6)_A$ $(7,7)_D$	$(10)_A$ $(10)_D$
ANFIS	Membership functions: 2 Necessary iterations: 10 Type of membership functions: Generalized bell-shaped membership function		
ARIMA	p = 6, d = 0, q = 5		

[a] Neural network structure $(x, y)_z$: x and y represent the number of neurons in one and two layers, respectively; z represents the approximation or detail series of the wavelet decomposition.

leading to unrealistic discontinuities. In reality, however, a *Chl a* time series shows some aspects of continuous behavior.

Fortunately, WNARNet can provide a good balance between the cumulative errors and the correlations between the steps, leading to the best performance in multistep- ahead forecasting of the Chl *a* series.

Second, the importance of discrete wavelet transform was analyzed. As shown in Fig. 7, the performance of WNARNet is much better than that of NAR. In WNARNet, the original series (S) is decomposed into two subseries (A & D) by the discrete wavelet transform introduced in Section 2.2.2, meaning that the forecasting process is carried out by a two-pathway NAR. Each one-step-ahead forecast of A & D will produce two values after the reconstruction of the original series. Therefore, for the same horizon, the cumulative number of WNARNet is halved relative to that of NAR, thereby reducing the accumulated error and improving the accuracy of the long-term forecast. Combining the wavelet transform with NAR achieves a tremendous improvement, as shown in Table 4, Figs. 6, and 7.

However, the forecasting results of ANN are slightly better than those of WNN. For both r and RMSE, the curves for ANN and WNN are very close (Fig. 7). Since both models are direct strategy methods, for each step-ahead forecast, ANN needs to train a new network, which is not feasible in practice. On the other hand, WNN can forecast two values in one shot, similar to WNARNet, and needs to train two new networks for each one-step-ahead forecast. Therefore, for the same horizon, ANN and WNN need to train the same number of networks,

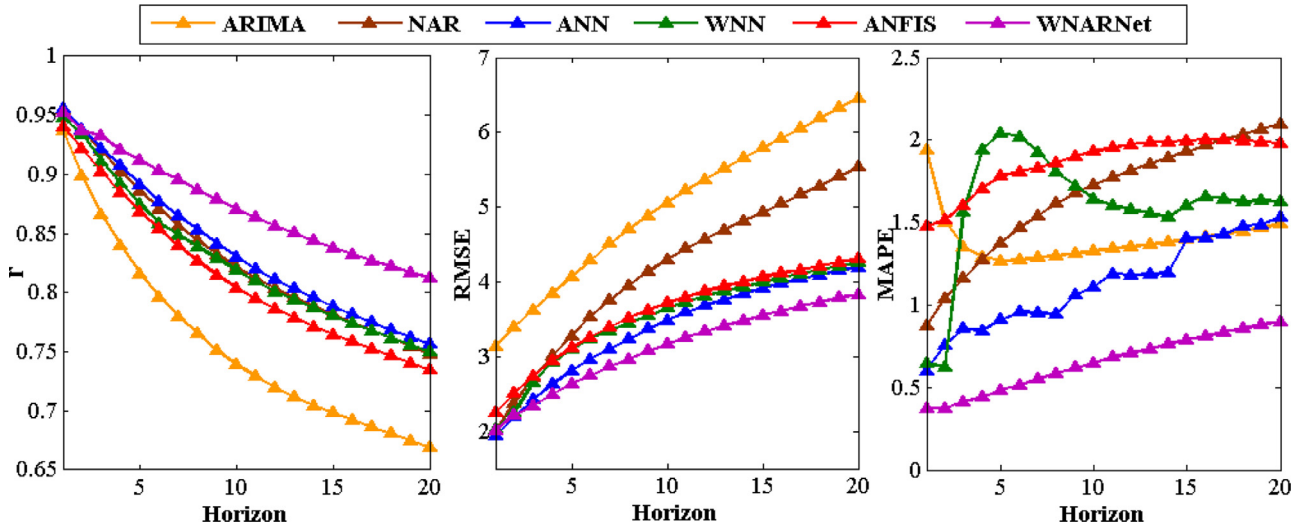

Fig. 6. Comparison of the predictive performance of the different models with different horizons.

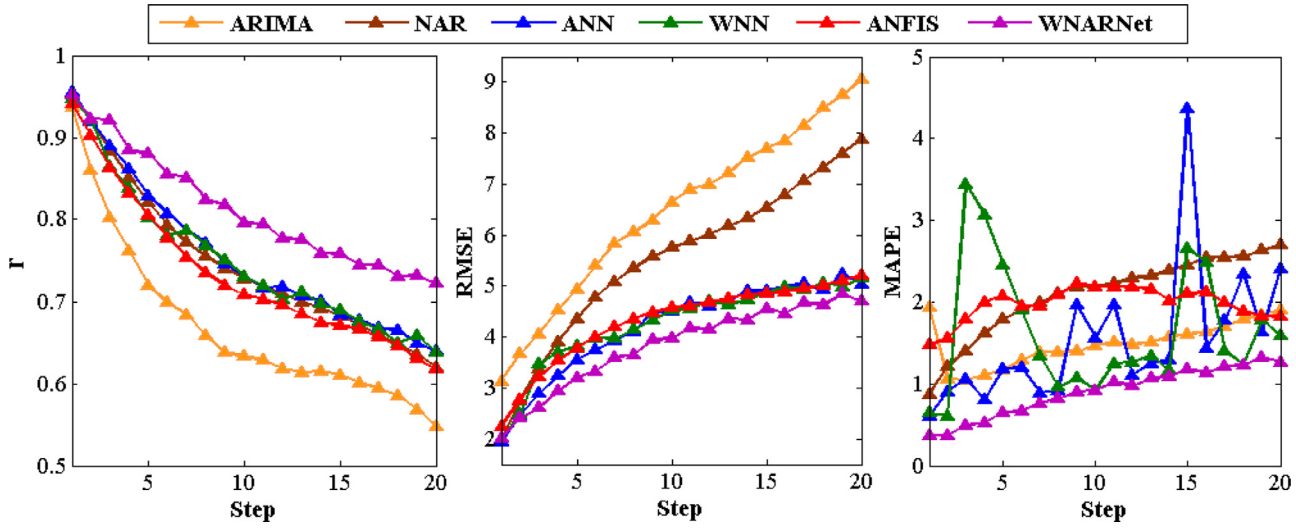

Fig. 7. Comparison of the predictive performance of the different models at each step for a horizon of 20.

and the results are similar.

3.4. Statistical analysis

Statistical tests are used to examine the forecasting performance between the proposed model and others. Table 5 shows the results of the paired two-tailed *t*-tests, which indicate that the proposed WNARNet outperforms four (i.e., ARIMA, NAR, WNN and ANFIS) of the five approaches at a 5% statistical significance level. The paired two-tailed *t*-test shows that the predictions of the proposed model and ANN are equally accurate. Since *t*-test results are easily influenced by sample size [41], we calculate and compare the average RMSE for different forecasting horizons from 1 to 20. The proposed WNARNet has smaller average RMSE values than does ANN. In summary, statistical analysis demonstrates that WNARNet provides better forecasting performance than the other time series forecasting approaches.

4. Discussion

HABs are a matter of worldwide concern that have occurred with increasing frequency and range [42]. HAB events requiring restrictions on fisheries, recreation, and drinking-water uses of inland water bodies lead to significant economic consequences [43]. *Chl a* is an important indicator of HABs, and forecasting the future *Chl a* concentrations is crucial for the early warning of HABs. Therefore, it is imperative to develop advanced models to forecast *Chl a* multiple steps ahead continuously.

With the development of monitoring equipment, especially online automatic instruments [44], the volume and the quality of data have been greatly improved, providing long-term datasets with a high time resolution. However, when the HABs occur, the time series of *Chl a* usually has a large number of mutations, implying that the series is nonstationary. The multistep-ahead forecasting model developed in this study, which combines the discrete wavelet transform with NARs, can better address the challenges caused by the non-stationarity. The advantages of integrating discrete wavelet transform are twofold: First, the decomposition process can extract the noises, trends and hidden laws of the signal by transforming the original series into different frequencies. Second, the forecasting process of a decomposed series is parallel so that the accumulated errors of the recursive strategy can be significantly reduced. Therefore, the approach using a decomposed series (i.e., WNARNet) performs better than the other recursive strategy approaches that directly use the original data (i.e., NAR and ARIMA), as indicated by the smaller forecasting errors.

Compared to the direct strategy approaches (i.e., ANN, ANFIS and WNN), the approach proposed in this study is more extensible and

Table 4
Evaluation and comparison of the different models for the multistep forecasting of *Chl a*.

Algorithm	*h*th step (horizon = 20)[a]			Horizon[b]		
	r	RMSE (μg L^{-1})	MAPE	r	RMSE (μg L^{-1})	MAPE
ARIMA						
1	0.937	3.133	1.941	0.937	3.133	1.941
10	0.633	6.647	1.467	0.739	5.057	1.704
20	0.548	9.053	1.909	0.669	6.462	1.772
ANN						
1	**0.956**	1.934	0.603	0.956	1.934	0.603
10	0.731	4.503	1.565	0.830	3.485	1.084
20	0.639	5.044	2.402	0.756	4.196	1.523
NAR						
1	**0.954**	2.006	0.871	0.954	2.006	0.871
10	0.727	5.760	2.184	0.822	4.298	1.528
20	0.620	7.877	2.700	0.748	5.532	1.919
WNN						
1	0.948	2.020	0.644	0.948	2.020	0.644
10	0.731	4.525	0.918	0.819	3.646	0.781
20	0.638	5.152	1.583	0.750	4.254	1.048
ANFIS						
1	0.941	2.247	1.478	0.941	2.247	1.478
10	0.709	4.576	2.189	0.804	3.719	1.833
20	0.617	5.211	1.822	0.734	4.306	1.829
WNAR						
1	**0.952**	**2.010**	**0.375**	**0.952**	**2.010**	**0.375**
10	**0.795**	**3.975**	**0.920**	**0.871**	**3.167**	**0.648**
20	**0.722**	**4.696**	**1.266**	**0.812**	**3.829**	**0.854**

[a] Comparison of 1st, 10th and 20th step forecasting performance of different models when horizon is 20.
[b] Comparison of forecasting performance of different models with different horizons (H = 1,10 and 20).

Table 5
The results of statistical tests.

Compared Algorithms	Paired 2-tailed *t*-tests with WNARNet (avg. RMSE = 3.109)[a]		
	p-Value	*t*-Statistic	avg. RMSE
ARIMA	0.0000	−7.285	5.001
NAR	0.0003	−3.936	4.149
ANN	**0.1919**	−1.329	3.371
WNN	0.0391	−2.137	3.516
ANFIS	0.0130	−2.608	3.590

[a] Confidence level $\alpha = 0.05$.

reusable. Because the approaches based on the direct strategy require the training of new models for each step prediction, they consume a large quantity of computing resources and time. In contrast, WNARNet is capable of forecasting different horizons with the same model.

Moreover, the correlation of the forecasted *Chl a* values is critical to illustrating the future trends of the whole series. As a recursive-joint strategy method, WNARNet retains the relationships in the forecasted series by using the previous forecasted values as the input to forecast the latter values. For the direct strategy, the values are predicted in isolation, suggesting that the relationship between the values are lost. This again supports our proposition that the WNARNet approach may be a useful method for multistep-ahead forecasting of *Chl a*.

In our study, WNARNet was successfully verified using real data of the Wenzhou coastal area. The model reliably predicted the *Chl a* concentration 20 steps ahead. The powerful ability to express these relationships suggests the potential of this model to predict not only the *Chl a* series but also other nonstationary series. However, due to the limited available data, this multistep-ahead forecasting model has only been successfully applied in one case area. Further research will be focused on testing the wide practicality and generalization of this multistep-ahead forecasting model.

5. Conclusions

An effective multistep-ahead forecasting model, WNARNet, is proposed in this study to predict *Chl a* concentration. The wavelet transform is applied to decompose the original series into two different frequencies to alleviate the difficulty of model fitting and to improve the performance. Due to the use of the recursive strategy of NAR, the correlations between time series are retained. Based on all the above, the buoy monitoring data during 2014-2015 from the Wenzhou coastal area is used as the experimental dataset. The proposed WNARNet is applied to forecast *Chl a* multiple steps ahead and obtains a high accuracy. Compared to other multistep-ahead forecasting methods, the WNARNet developed in this study has better prediction accuracy. Moreover, the model can forecast different horizons flexibly and can be scaled with a simple structure, demonstrating that the model has good feasibility and effectiveness. The current model requires hourly data for effectively and flexibly forecasting *Chl a*. However, for different monitoring equipment and situations, the monitoring frequency may be higher (e.g., minutes or seconds) or lower (e.g., daily or weekly). Therefore, future research efforts will focus on further development of the model to enable its use with datasets of different time resolutions.

Acknowledgments

This research was supported by the National Key Research and Development Program of China under Grant 2018YFB0505004, Public Science and Technology Research Funds' Projects (201305012, 201505003) and the Fundamental Research Funds for the Central Universities from Ministry of Education of the People's Republic of China under grant number 2016XZZX004-02.

Supplementary materials

Supplementary material associated with this article can be found, in the online version, at doi:10.1016/j.knosys.2018.06.015.

References

[1] B.E. Lapointe, L.W. Herren, D.D. Debortoli, M.A. Vogel, Evidence of sewage-driven eutrophication and harmful algal blooms in Florida's Indian River Lagoon, Harmful Algae 43 (2015) 82–102, https://doi.org/10.1016/j.hal.2015.01.004.
[2] K.E. Havens, H. Paerl, Climate change at a crossroad for control of harmful algal blooms, Environ. Sci. Technol. (2015), https://doi.org/10.1021/acs.est.5b03990.
[3] H.W. Paerl, W.S. Gardner, K.E. Havens, A.R. Joyner, M.J. Mccarthy, S.E. Newell, B. Qin, J.T. Scott, Mitigating cyanobacterial harmful algal blooms in aquatic ecosystems impacted by climate change and anthropogenic nutrients, Harmful Algae 54 (2016) 213–222, https://doi.org/10.1016/j.hal.2015.09.009.
[4] M. Qin, Z. Li, Z. Du, Red tide time series forecasting by combining ARIMA and deep belief network, Knowledge-Based Syst. 125 (2017) 39–52, https://doi.org/10.1016/j.knosys.2017.03.027.
[5] Q. Chen, T. Guan, L. Yun, R. Li, F. Recknagel, Online forecasting chlorophyll a concentrations by an auto-regressive integrated moving average model: Feasibilities and potentials, Harmful Algae 43 (2015) 58–65, https://doi.org/10.1016/j.hal.2015.01.002.
[6] X. Xiao, J. He, H. Huang, T.R. Miller, G. Christakos, E.S. Reichwaldt, A. Ghadouani, S. Lin, X. Xu, J. Shi, A novel single-parameter approach for forecasting algal blooms, Water Res. 108 (2017) 222–231, https://doi.org/10.1016/j.watres.2016.10.076.
[7] Y. Kim, H.S. Shin, J.D. Plummer, A wavelet-based autoregressive fuzzy model for forecasting algal blooms, Environ. Model. Softw. 62 (2014) 1–10, https://doi.org/10.1016/j.envsoft.2014.08.014.
[8] A. Sorjamaa, J. Hao, N. Reyhani, Y. Ji, A.L. Ã, Methodology for long-term prediction of time series, Neurocomputing 70 (2007) 2861–2869, https://doi.org/10.1016/j.neucom.2006.06.015.
[9] S. Ben Taieb, G. Bontempi, A.F. Atiya, A. Sorjamaa, A review and comparison of strategies for multi-step ahead time series forecasting based on the NN5 forecasting competition, Expert Syst. Appl. 39 (2012) 7067–7083, https://doi.org/10.1016/j.eswa.2012.01.039.
[10] S. Ben Taieb, A.F. Atiya, S. Member, A bias and variance analysis for multistep-ahead time series forecasting, IEEE Trans. Neural Netw. Learn. Syst. 27 (2016) 62–76.
[11] S.V. Kumar, L. Vanajakshi, Short-term traffic flow prediction using seasonal ARIMA

model with limited input data, Eur. Transp. Res. Rev. 7 (2015) 1–9, https://doi.org/10.1007/s12544-015-0170-8.
[12] K. Hatalis, P. Pradhan, S. Kishore, R.S. Blum, A.J. Lamadrid, Multi-step forecasting of wave power using a nonlinear recurrent neural network, PES Gen. Meet. Conf. Expo. 2014 IEEE, 2014, pp. 1–5.
[13] T. Nanda, B. Sahoo, H. Beria, C. Chatterjee, A wavelet-based non-linear auto-regressive with exogenous inputs (WNARX) dynamic neural network model for real-time flood forecasting using satellite-based rainfall products, J. Hydrol. 539 (2016) 57–73, https://doi.org/10.1016/j.jhydrol.2016.05.014.
[14] K. Benmouiza, A. Cheknane, Small-scale solar radiation forecasting using ARMA and nonlinear autoregressive neural network models, Theor. Appl. Climatol. 124 (2016) 945–958, https://doi.org/10.1007/s00704-015-1469-z.
[15] T. Zhou, S. Gao, J. Wang, C. Chu, Y. Todo, Z. Tang, Financial time series prediction using a dendritic neuron model, Knowledge-Based Syst. 105 (2016) 214–224, https://doi.org/10.1016/j.knosys.2016.05.031.
[16] B. Doucoure, K. Agbossou, A. Cardenas, Time series prediction using artificial wavelet neural network and multi-resolution analysis : application to wind speed data, Renew. Energy 92 (2016) 202–211, https://doi.org/10.1016/j.renene.2016.02.003.
[17] I. Aizenberg, L. Sheremetov, L. Villa-Vargas, Multilayer neural network with multi-valued neurons in time series forecasting of oil production, Neurocomputing 175 (2016) 980–989, https://doi.org/10.1007/978-3-319-07491-7_7.
[18] P.-C. Chang, J.-L. Wu, J.-J. Lin, A Takagi–Sugeno fuzzy model combined with a support vector regression for stock trading forecasting, Appl. Soft Comput. 38 (2016) 831–842, https://doi.org/10.1016/j.asoc.2015.10.030.
[19] G.J. Osório, J.C.O. Matias, J.P.S. Catalão, Short-term wind power forecasting using adaptive neuro-fuzzy inference system combined with evolutionary particle swarm optimization, wavelet transform and mutual information, Renew. Energy 75 (2015) 301–307, https://doi.org/10.1016/j.renene.2014.09.058.
[20] J.S.R. Jang, ANFIS: adaptive-network-based fuzzy inference system, IEEE Trans. Syst. Man Cybern. 23 (1993) 665–685, https://doi.org/10.1109/21.256541.
[21] R. Barzegar, E. Fijani, A. Asghari, E. Tziritis, Forecasting of groundwater level fluctuations using ensemble hybrid multi-wavelet neural network-based models, Sci. Total Environ. 599–600 (2017) 20–31, https://doi.org/10.1016/j.scitotenv.2017.04.189.
[22] D. Wang, S. Wei, H. Luo, C. Yue, O. Grunder, A novel hybrid model for air quality index forecasting based on two-phase decomposition technique and modified extreme learning machine, Sci. Total Environ. 580 (2017) 719–733, https://doi.org/10.1016/j.scitotenv.2016.12.018.
[23] P. Wang, Y. Liu, Z. Qin, G. Zhang, A novel hybrid forecasting model for PM10 and SO2 daily concentrations, Sci. Total Environ. 505 (2015) 1202–1212, https://doi.org/10.1016/j.scitotenv.2014.10.078.
[24] J.L. Salmeron, W. Froelich, Dynamic optimization of fuzzy cognitive maps for time series forecasting, Knowledge-Based Syst 105 (2016) 29–37, https://doi.org/10.1016/j.knosys.2016.04.023.
[25] F. Shen, J. Chao, J. Zhao, Forecasting exchange rate using deep belief networks and conjugate gradient method, Neurocomputing 167 (2015) 243–253, https://doi.org/10.1016/j.neucom.2015.04.071.
[26] P. Jiang, X. Liu, J. Zhang, X. Yuan, A framework based on hidden Markov model with adaptive weighting for microcystin forecasting and early-warning, Decis. Support Syst. 84 (2016) 89–103, https://doi.org/10.1016/j.dss.2016.02.003.
[27] N. An, W. Zhao, J. Wang, D. Shang, E. Zhao, Using multi-output feedforward neural network with empirical mode decomposition based signal filtering for electricity demand forecasting, Energy 49 (2013) 279–288, https://doi.org/10.1016/j.energy.2012.10.035.
[28] Z. Hu, Y. Bao, R. Chiong, T. Xiong, Mid-term interval load forecasting using multi-output support vector regression with a memetic algorithm for feature selection, Energy 84 (2015) 419–431, https://doi.org/10.1016/j.energy.2015.03.054.
[29] T. Xiong, Y. Bao, Z. Hu, Multiple-output support vector regression with a firefly algorithm for interval-valued stock price index forecasting, Knowledge-Based Syst. 55 (2014) 87–100, https://doi.org/10.1016/j.knosys.2013.10.012.
[30] D. Letson, D. Solı, Assessing the value of climate information and forecasts for the agricultural sector in the Southeastern United States : multi-output stochastic frontier approach, 13 (2013) 5–14. doi:10.1007/s10113-012-0354-x.
[31] X.U. Hai-long, G.U. De-xian, Z. Wen-liang, G.A.O. Qi, Q. Xiu-ting, Time series analysis of red tide's disaster characteristics in China seas, Mar. Sci. Bull. 17 (2015) 1–10.
[32] S.G. Mallat, A theory for multiresolution signal decomposition: the wavelet representation, IEEE Trans. Pattern Anal. Mach. Intell. 11 (1989) 674–693, https://doi.org/10.1109/34.192463.
[33] L. Pasti, B. Walczak, D.L. Massart, P. Reschiglian, Optimization of signal denoising in discrete wavelet transform, Chemom. Intell. Lab. Syst. 48 (1999) 21–34.
[34] D. Gupta, S. Choubey, Discrete wavelet transform for image processing, Int. J. Emerg. Technol. Adv. Eng. 4 (2008) 598–602.
[35] R. Quiroz, C. Yarlequé, A. Posadas, V. Mares, W.W. Immerzeel, Improving daily rainfall estimation from NDVI using a wavelet transform, Environ. Model. Softw. 26 (2011) 201–209, https://doi.org/10.1016/j.envsoft.2010.07.006.
[36] R. Singh, A. Khare, Fusion of multimodal medical images using Daubechies complex wavelet transform – A multiresolution approach, Inf. Fusion. 19 (2014) 49–60, https://doi.org/10.1016/j.inffus.2012.09.005.
[37] K. Benmouiza, A. Cheknane, Forecasting hourly global solar radiation using hybrid k-means and nonlinear autoregressive neural network models, Energy Convers. Manag. 75 (2013) 561–569, https://doi.org/10.1016/j.enconman.2013.07.003.
[38] S. Ferlito, M. Atrigna, G. Graditi, S. De Vito, M. Salvato, A. Buonanno, G. Di Francia, Predictive models for building's energy consumption: an Artificial Neural Network (ANN) approach, AISEM Annu. Conf. 2015 XVIII, 2015, pp. 3–6.
[39] T. Leung, Nonlinear autoregressive integrated neural network del for short-term load forecasting, IEEE Proceedings-Generation, Transm. Distrib. 143 (1996) 500–506.
[40] P. Coad, B. Cathers, J.E. Ball, R. Kadluczka, Proactive management of estuarine algal blooms using an automated monitoring buoy coupled with an artificial neural network, Environ. Model. Softw. 61 (2014) 393–409, https://doi.org/10.1016/j.envsoft.2014.07.011.
[41] M.Y. Chen, B.T. Chen, A hybrid fuzzy time series model based on granular computing for stock price forecasting, Inf. Sci. (Ny). 294 (2015) 227–241, https://doi.org/10.1016/j.ins.2014.09.038.
[42] A. Silva, L. Pinto, S.M. Rodrigues, H. De Pablo, M. Santos, T. Moita, M. Mateus, A HAB warning system for shellfish harvesting in Portugal, Harmful Algae 53 (2016) 33–39, https://doi.org/10.1016/j.hal.2015.11.017.
[43] B.W. Brooks, J.M. Lazorchak, M.D.A. Howard, M.-V.V. Johnson, S.L. Morton, D.A.K. Perkins, E.D. Reavie, G.I. Scott, S.A. Smith, J.A. Steevens, Are harmful algal blooms becoming the greatest inland water quality threat to public health and aquatic ecosystems? Environ. Toxicol. Chem. 35 (2016) 6–13, https://doi.org/10.1002/etc.3220.
[44] H. Shibata, A study of the red-tide monitoring system using drifting buoy and wireless networks, Proc. Twenty-Fifth Int. Ocean Polar Eng. Conf. 2015, pp. 1132–1138.